

Phase variation of hadronic amplitudes

J.-P. Dedonder

Université Paris Diderot-Paris 7, IMNC/Case 7021 Bâtiment Condorcet, F-75205 Paris cedex 13, France

W. R. Gibbs

New Mexico State University, Las Cruces, New Mexico 88003, USA

Mutazz Nuseirat

King Saud Bin Abdulaziz University, P.O. Box 22490, Riyadh 11426, Kingdom of Saudi Arabia

(Received 3 December 2007; published 11 April 2008)

The phase variation with angle of hadronic amplitudes is studied with a view to understanding the underlying physical quantities that control it and how well it can be determined in free space. We find that unitarity forces a moderately accurate determination of the phase in standard amplitude analyses but that the nucleon-nucleon analyses done to date do not give the phase variation needed to achieve a good representation of the data in multiple scattering calculations. Models are examined that suggest its behavior near forward angles is related to the radii of the real and absorptive parts of the interaction. The dependence of this phase on model parameters is such that if these radii are modified in the nuclear medium (in combination with the change due to the shift in energy of the effective amplitude in the medium) then the larger magnitudes of the phase needed to fit the data might be attainable but only for negative values of the phase variation parameter.

DOI: [10.1103/PhysRevC.77.044003](https://doi.org/10.1103/PhysRevC.77.044003)

PACS number(s): 21.45.Bc, 13.75.Jz, 25.55.Ci

I. INTRODUCTION

A phenomenological form often used for the nucleon-nucleon scattering amplitude is

$$f_{ph}(q) = \frac{ik\sigma(1-i\rho)}{4\pi} e^{-\frac{1}{2}aq^2}, \quad a = a_R + ia_I, \quad (1)$$

where σ is the total cross section and ρ is the ratio of the real to imaginary part of the forward amplitude. This latter can be measured by interference with the coulomb amplitude. The parameter a_R can be extracted from the falloff of the cross section. At a common value at the beam momentum we will consider here (1.75 GeV/c) it is usually taken to be $5.6 (\text{GeV}/c)^{-2}$. The parameter a_I has often been assumed to be zero for lack of better knowledge.

Although the variation of the phase of the nucleon-nucleon amplitude with momentum transfer had been considered before [1,2], in seminal articles Franco and Yin [3] found that the value of a_I strongly influenced multiple scattering in light nuclei and they were able to obtain a much better representation of the data if they treated it as a free parameter. The values that they found were $+10 (\text{GeV}/c)^{-2}$ and $-15 (\text{GeV}/c)^{-2}$ with either value giving a dramatic improvement in the agreement with the data. They considered α -particle scattering from ^4He , ^3He , deuterium, and ^1H and found the same improvement for all targets with the same values of a_I . This, and other studies of multiple scattering [4–9], will be discussed in Sec. VI.

In an attempt to estimate reasonable theoretical values for a_I , Ahmad and Alvi [10] studied an eikonal [11] approximation based on an effective potential and concluded that a_I should be expected to have a magnitude of the order of $1 (\text{GeV}/c)^{-2}$ or less, apparently in disagreement with the previous work.

However, Ref. [10] considered a potential in which the real and imaginary parts had the same spatial distribution, a Gaussian form being taken for each component. It is generally believed that the nucleon-nucleon interaction is more complicated than this and that the ranges to be associated with the different parts of the interaction (real and imaginary) are significantly different.

A principal aim of this article is to investigate the effect of assuming what is hoped are reasonable estimates for the forms of the potential and to understand the relationship of the parameter a_I to the geometric structure of the interaction.

We will often follow the eikonal method used by Ref. [10]. In this approximation one can write

$$f_{ei}(q) = \frac{ik}{2\pi} \int d^2b e^{iq \cdot b} \Gamma(b) = ik \int_0^\infty b db J_0(qb) \Gamma(b), \quad (2)$$

where

$$\Gamma(b) = 1 - e^{i\chi(b)} \quad \text{and} \quad \chi(b) = -\frac{1}{\hbar v} \int_{-\infty}^\infty V(\sqrt{b^2 + z^2}) dz, \quad (3)$$

$V(r)$ is a complex potential and J_0 is the Bessel function of zero order.

To obtain the forward angle dependence of the phase we can expand Eq. (2) in powers of q and equate the coefficients of q^0 and q^2 in the second-order expansion of these expressions with the expansion of Eq. (1) to find

$$a = \frac{1}{2} \frac{\int_0^\infty b^3 \Gamma(b) db}{\int_0^\infty b \Gamma(b) db}. \quad (4)$$

We observe that there is a symmetry that exists in these expressions. If the sign of the real part of the potential

is changed ($V_{\text{Real}} \rightarrow -V_{\text{Real}}$), then $\Gamma(b) \rightarrow \Gamma^*(b)$, which means that $\rho \rightarrow -\rho$ and $a_I \rightarrow -a_I$.

We proceed in the remainder of the article to investigate the origin and dependencies of the phase of the strong scattering amplitude. In Sec. II we introduce the relationship of the phase to the difference in interaction ranges with a schematic model. This model, crude as it is, gives us some indication of the interdependencies among the physical quantities and the underlying physics involved.

In Sec. III we look at the conditions imposed by unitarity on the phase and its determination from phase-shift analyses. We investigate the accuracy to which the phase can be determined in a typical realistic (K^+p) case. In Sec. IV we show the results of the NN analysis by Arndt *et al.* [12].

In Sec. V we investigate three potential models to give a somewhat more realistic evaluation of the interdependence among the parameters and their variation with energy. Section VI treats the question of determining the phase variation parameter a_I from multiple scattering. In Sec. VII we draw conclusions from the work and discuss the possible changes of the phase in the medium due to nucleonic and non-nucleonic mechanisms.

II. SCHEMATIC DELTA FUNCTION MODEL

As a first orientation, let us consider a schematic model in which the strength of the integrand in Eq. (2) is concentrated at points in the impact parameter variable, b . To see the connection between the phase and the radii of the real and imaginary parts of the interaction it is useful to define a slightly modified amplitude such that the imaginary part is equal to the total cross section

$$F(q) = \frac{4\pi}{k} f(q) \quad \text{along with} \quad G(b) = 4\pi i \Gamma(b) \quad (5)$$

so that Eq. (2) becomes

$$F(q) = \frac{1}{2\pi} \int d^2 b e^{i\mathbf{q}\cdot\mathbf{b}} G(b). \quad (6)$$

Note that

$$F(0) = \sigma(\rho + i). \quad (7)$$

We now wish to investigate the assumption that the real and imaginary parts of the strength of $G(b)$ are concentrated in different regions of impact parameters, hence we consider the simple model in which the distribution of the strength of $G(b)$ is expressed by δ functions, i.e., we take

$$G(b) = G_R \delta(b - b_R) + i G_I \delta(b - b_I). \quad (8)$$

Now

$$F(0) = G_R b_R + i G_I b_I = \rho \sigma + i \sigma \quad (9)$$

so that the constants G_R and G_I are determined and we can write

$$G(b) = \sigma \left[\frac{\rho}{b_R} \delta(b - b_R) + i \frac{1}{b_I} \delta(b - b_I) \right], \quad (10)$$

which, using Eq. (4), leads to

$$a = a_R + i a_I = \frac{\rho b_R^2 + i b_I^2}{2(\rho + i)} \quad (11)$$

or

$$a_R = \frac{\frac{1}{2}(b_I^2 + \rho^2 b_R^2)}{1 + \rho^2}, \quad a_I = \frac{1}{2} \rho \left(\frac{b_I^2 - b_R^2}{1 + \rho^2} \right). \quad (12)$$

Thus we see that a_I is directly related to the difference in the radii of the real and imaginary parts.

If we assume that b_R is to be associated with one-pion exchange, dominant in this region of low momentum transfer [13], and the absorption radius with the two-pion exchange range [14], or about half as big, then, with a one-pion-exchange range of 1.4 fm we have,

$$\begin{aligned} \frac{1}{2}(b_I^2 - b_R^2) &= \frac{1}{2}(0.7^2 - 1.4^2) \text{ fm}^2 = -0.75 \text{ fm}^2 \\ &\approx -19.3 (\text{GeV}/c)^{-2} \end{aligned} \quad (13)$$

so that a_I is roughly proportional to ρ (for small values) with a relatively large coefficient. If we were to take the two radii to be equal (as was done in Ref. [10]) the coefficient would be zero. We also see a strong correlation between a_I and ρ . We will see later that these general features are present in more realistic potential models. The relation between the phase and impact parameters has been discussed before [15], although at much higher energies ($P_{\text{Lab}} \geq 100 \text{ GeV}/c$).

III. UNITARY CONSTRAINTS

We now investigate to what extent the fact that physical amplitudes have an expression in partial waves with coefficients that satisfy unitary constraints restricts the phase parameter a_I . The constraint of unitarity on the amplitudes, and in particular the phase, has been studied for some time. Gerber and Karplus [16] showed that unitarity could be a strong constraint. More recently Huber *et al.* [17] studied the spin 1/2 on spin 0 scattering system below inelastic threshold. They find (apart from discrete ambiguities that disappear with the measurement of polarization and the determination of the sign of the real part of the non-spin-flip amplitude at one energy) that the phase is indeed determined from unitarity considerations. In the present case we are treating a moderately inelastic scattering system. Although one might worry about additional ambiguities arising in this case, we point out that the reaction data are also available (and used in our analysis), which can be expected to help. We also are not allowing a general phase variation but only a linear (in $\cos \theta$) variation in the forward direction. We first consider the model amplitude in Eq. (1) and then go on to treat the general case.

A. Unitary limits for a Gaussian amplitude

In the form used in Eq. (1) there are limits on the values a_R and a_I can take from a unitary expansion of the amplitude, assuming the amplitude represents scattering of a zero-spin projectile on a zero-spin target. We can write

$$\begin{aligned} &\frac{ik\sigma(1-i\rho)}{4\pi} e^{-\frac{1}{2}aq^2} \\ &= \frac{ik\sigma(1-i\rho)}{4\pi} e^{-ak^2} \sum_{\ell=0}^{\infty} i^\ell (2\ell+1) j_\ell(-iak^2) P_\ell(x) \\ &= \frac{1}{2ik} \sum_{\ell=0}^{\infty} (2\ell+1) (S_\ell - 1) P_\ell(x), \end{aligned} \quad (14)$$

where

$$q^2 = 2k^2(1 - x) \quad (15)$$

and $x = \cos \theta$. Thus, we can identify

$$S_\ell = 1 - \frac{k^2 \sigma (1 - i\rho)}{2\pi} e^{-ak^2} i^\ell j_\ell(-iak^2). \quad (16)$$

The fact that the absolute values of S_ℓ cannot exceed unity leads to the condition

$$1 \geq |S_\ell|^2 = 1 - 2\mu(R_\ell + \rho I_\ell) + \mu^2(1 + \rho^2)(R_\ell^2 + I_\ell^2), \quad (17)$$

where

$$\mu = \frac{k^2 \sigma}{2\pi} \quad (18)$$

and

$$R_\ell = \text{Re}[i^\ell e^{-ak^2} j_\ell(-iak^2)], \quad I_\ell = \text{Im}[i^\ell e^{-ak^2} j_\ell(-iak^2)]. \quad (19)$$

For a real ($= a_R$), so that $I_\ell = 0$, we can write the condition (17) as

$$\mu R_\ell \leq \frac{2}{1 + \rho^2}, \quad (20)$$

where R_ℓ is the real quantity $i^\ell e^{-a_R k^2} j_\ell(-ia_R k^2)$. Although this condition must hold for all partial waves, numerical studies indicate that the S -wave unitarity is the most likely to be violated. For this case we have the result

$$1 - e^{-2a_R k^2} \leq \frac{8\pi a_R}{\sigma(1 + \rho^2)}, \quad (21)$$

which can be regarded as a constraint on a_R or ρ .

This condition is similar to, but stronger than, the constraint arising from the requirement that the integrated elastic cross section is less than or equal to the total cross section, which is

$$1 - e^{-4a_R k^2} \leq \frac{16\pi a_R}{\sigma(1 + \rho^2)}. \quad (22)$$

With values of a_R satisfying the condition given by Eq. (20) we included finite values of a_I and studied numerically the resulting values of $|S_\ell|^2$. It was found that for values corresponding to large partial waves (where $|S_\ell|$ is nearly unity in any case), unitarity was violated to some (often small) extent.

We can see in the following that, in the limit of large ℓ , unitarity in some partial waves must be violated. Using the limit for large ℓ for the spherical Bessel function

$$\begin{aligned} i^\ell e^{-ak^2} j_\ell(-iak^2) &\longrightarrow \sqrt{\frac{e}{2}} i^\ell e^{-ak^2} \frac{(-iak^2 e)^\ell}{(2\ell + 1)^{\ell+1}} \\ &= \sqrt{\frac{e}{2}} e^{-ak^2} (a_R k^2 e)^\ell \frac{(1 + ia_I/a_R)^\ell}{(2\ell + 1)^{\ell+1}} \\ &\longrightarrow \sqrt{\frac{e}{2}} \frac{(a_R k^2 e)^\ell e^{-a_R k^2}}{(2\ell + 1)^{\ell+1}} e^{i\chi_\ell}, \end{aligned} \quad (23)$$

where

$$\chi_\ell \equiv -a_I k^2 + \ell \frac{a_I}{a_R}. \quad (24)$$

Because R_ℓ and I_ℓ are going to zero with increasing ℓ we can drop the last term in Eq. (17) to get

$$1 \geq 1 - \sqrt{2e\mu} \frac{(a_R k^2 e)^\ell e^{-a_R k^2}}{(2\ell + 1)^{\ell+1}} [\cos \chi_\ell + \rho \sin \chi_\ell]. \quad (25)$$

Because for some values of ℓ the quantity in brackets must be negative, we see that the condition will be violated for some S -matrix elements.

One important caveat is that this proof holds only for the scattering of two spin-zero particles because only in that case can the amplitude be written in the unitarity form we have taken. The Gaussian expression for the amplitude is often used for a spin-averaged amplitude that is not expressible in this form.

Thus, for the strict respect of unitarity, the form of Eq. (1) requires that $a_I \equiv 0$ and that condition (20) holds. Of course, one could modify the values of S_ℓ in any partial wave in which unitarity did not hold [i.e., so that Eq. (16) is no longer true] but the manner of carrying out this correction is nonunique and the functional form differs (perhaps only slightly) from Eq. (1). We discuss this problem from a more general point of view in the next section.

B. Unitary limits in amplitude analyses

A similar technique to that used in the previous section can be applied to a more general amplitude. We are particularly interested here in the use of a partial-wave expansion to represent experimental data and the question of how well the phase is determined.

To this end, we first consider the case, again, for spin-zero on spin-zero scattering, where one attempts to change the phase of the amplitude by an arbitrary function, $\phi(\theta)$, to obtain an amplitude with a different phase:

$$\tilde{f}(\theta) = e^{i\phi(\theta)} f(\theta). \quad (26)$$

It has often been assumed that such a phase would be undetectable in elastic scattering because it does not affect the measurable cross section. It does, however, modify unitarity in a manner similar to that seen in the previous section.

We will take the form of $\phi(\theta)$ to be linear in t , i.e.,

$$\phi(\theta) = -\frac{1}{2}\delta a_I t = \frac{1}{2}\delta a_I 2k^2(1 - \cos \theta), \quad (27)$$

where $\nu = \delta a_I k^2$. We can expand both amplitudes in Eq. (26) in Legendre series to find

$$f(\theta) = \sum_\ell f_\ell P_\ell(\cos \theta) \quad \text{and} \quad \tilde{f}(\theta) = \sum_L \tilde{f}_L P_L(\cos \theta), \quad (28)$$

where

$$f_\ell = \frac{S_\ell - 1}{2ik} \quad \text{and} \quad \tilde{f}_L = \frac{\tilde{S}_L - 1}{2ik}. \quad (29)$$

Using Bauer's series,

$$e^{-i\nu x} = \sum_\lambda i^\lambda (2\lambda + 1) P_\lambda(\cos \theta) j_\lambda(-\nu), \quad (30)$$

and Eqs. (26), (27), and (28), we can express the coefficients in the expansion of $\tilde{f}(\theta)$ as

$$\tilde{f}_L = e^{i\nu} \sum_{\lambda, \ell} (2\lambda + 1) i^\lambda j_\lambda(-\nu) f_\ell [C_{L, \lambda, \ell}^{0,0,0}]^2, \quad (31)$$

where $C_{L_1, L_2, L_3}^{M_1, M_2, M_3}$ is a Clebsch-Gordon coefficient. Solving for the S -matrix element \tilde{S}_L from Eqs. (29) and (31) one can check if $|\tilde{S}_L|^2 \leq 1$. We find, with numerical studies, that unitarity is always violated in some partial wave.

How to judge the seriousness of a violation of unitarity is perhaps not obvious. One way to do so is to correct the violation and see what difference the change makes in the cross section and other observables derived from the new amplitude. This leads then to constraints due to the data. Rather than make *ad hoc* changes to the S -matrix elements, it is preferable to perform a search fitting the data to make the decision about how the parameters are to be changed to preserve unitarity, give the desired phase, and, at the same time, give the best fit to the data in the sense of a lowest χ^2 .

We have implemented this idea in a fitting program for K^+p scattering [18], a system for which the data are relatively good. The isospin structure is the same as in nucleon-nucleon scattering but the spin structure is less complex. For K^+p scattering there is no one-pion-exchange (OPE) contribution as there is in the nucleon-nucleon case. It has been suggested that OPE will help to determine the phase of the amplitude for NN scattering [19] but in the present test we have only the unitarity constraints to determine the phase.

We now study how well the phase can be determined in the process of finding a fit of a unitary form to the data. For K^+p scattering we can write the amplitude as $F(\theta) + \sigma \cdot \mathbf{n}G(\theta)$, where \mathbf{n} is a unit vector perpendicular to the scattering plane. In the course of this work a minimum lower than those found in Ref. [18] was observed. The original best χ^2 found was 2031.05, whereas the new one is at 2016.77. Although the difference in χ^2 per data point is very small, as is the change in the phase-shift parameters, the difference in χ^2 is important for the calculation of error estimates.

The procedure used is first to calculate the “natural” phase, ϕ_0 , obtained from the original fit to the experimental data. We then calculate a new phase, the “imposed” phase, $\phi = \phi_0 - \delta a_1 t$. In the fitting procedure, points from artificial data are included that consist of values of the phase to be imposed at a chosen single energy over a restricted range of t . The new phase “data” are included in the non-spin-flip amplitude, $F(\theta)$, only, the spin-flip amplitude being left free to have whatever phase the fit prefers. These additional phase “data” are taken to have very small errors to force the desired phase. A constant error (0.001 rad) is taken at each of five phase data points. In the modified minimization process there are two contributions to χ^2 :

$$\chi^2 = \chi_d^2 + \chi_\phi^2, \quad (32)$$

where χ_d^2 is the part of the χ^2 from the experimental data points and χ_ϕ^2 is that coming from the phase points.

The total χ^2 (including the phase data) is minimized but the part of χ^2 of principal interest is that due to the experimental data points, χ_d . It is found, as anticipated, that the χ_d^2 from

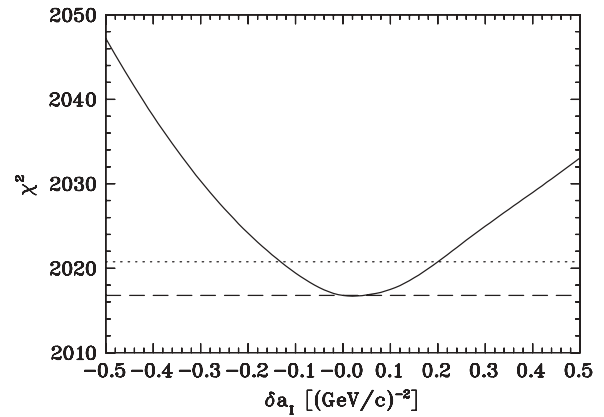


FIG. 1. Values of χ_d^2 as a function of the deviation of the phase from the original one. The dashed line indicates the minimum χ^2 and the dotted line is drawn at a value 4 units larger.

the true data increases as the imposed phase is chosen farther from the original phase, ϕ_0 .

The result of χ_d^2 for fitting the forward phase up to $-t = 0.32$ (GeV/c)² at a beam momentum of 1.3 GeV/c is shown in Fig. 1. An increase in χ_d^2 of 4 gives an estimate of the uncertainty of ± 0.2 (GeV/c)⁻².

In the upper part of Fig. 2 one sees that the imposed phase is well fit up to 0.4 (GeV/c)². Attempting to fit to a larger range of t did not lead to a better fit to the desired phase but instead the χ^2 due to the phase portion became larger. It appears that the limit has been reached where a modification of the phase linear in t can easily be used. The lower part of Fig. 2 shows the limits of ± 0.2 (GeV/c)⁻², an uncertainty of around $\pm 5\%$. Thus, the phase is reasonably well determined. One might believe that the phase of the nucleon-nucleon amplitude is better determined because of the use of OPE in the higher partial waves [19].

IV. NUCLEON-NUCLEON AMPLITUDE

With some confidence that a phase-shift fit to data provides a reasonably reliable determination of the absolute phase, we now turn to the nucleon-nucleon phase obtained from the recent fit by Arndt *et al.* [12]. The spin average is given by

$$\begin{aligned} \bar{M} &= \frac{1}{2} (\langle ++ | M | ++ \rangle + \langle +- | M | +- \rangle) \\ &= \frac{M_{11} + \frac{1}{2} M_{ss} + \frac{1}{2} M_{00}}{2}. \end{aligned} \quad (33)$$

The amplitude must also be averaged over the neutron and proton so that the averaged amplitude becomes

$$A = \frac{3}{4} \bar{M}(I = 1) + \frac{1}{4} \bar{M}(I = 0). \quad (34)$$

In Fig. 3 are shown several properties of the Arndt *et al.* [12] amplitudes at 1.8 GeV/c. The value of a_R can be extracted by averaging the amplitudes or the cross sections. The top panels show the result of the two methods compared with the exponential form given in Eq. (1). Figure 3(c) shows the variation of the phase from the forward value. It is seen that

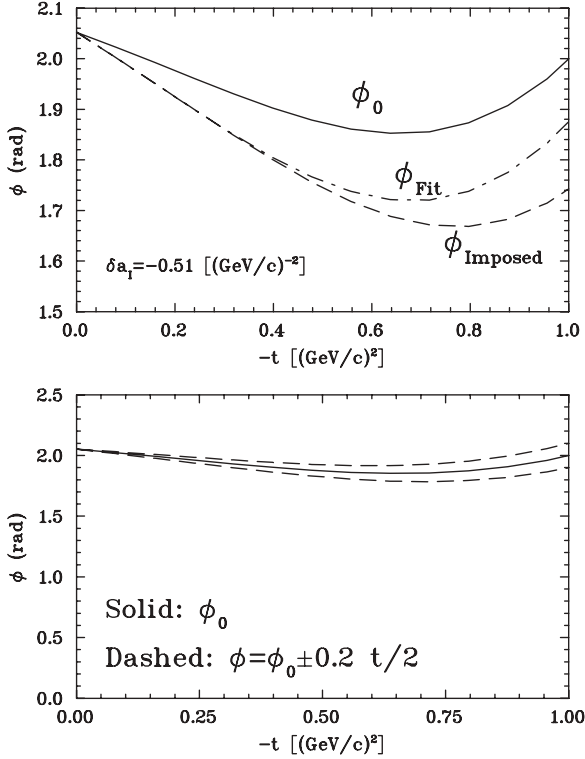


FIG. 2. Comparison of phases of $K^+ p$ scattering. (Upper panel) The solid curve gives the phase from the original amplitude and the dashed curve the result of modifying it with an additional phase with $\delta a_I = -0.51 \text{ (GeV/c)}^{-2}$. The dash-dot curve gives the phase of the amplitude resulting to the best fit to the experimental data plus the phase data out to 0.32 (GeV/c)^2 . The phases match out to about 0.36 (GeV/c)^2 . The case chosen for this comparison is the worst case (has the largest value of χ^2 from the phase “data”). (Lower panel) Original phase and limits corresponding to about two standard deviations in the classical estimate. The values that correspond to this point on Fig. 1 are about $\pm 0.2 \text{ (GeV/c)}^{-2}$.

a linear approximation in t is reasonable up to $-t$ of about 0.2 (GeV/c)^2 . Figure 3(d) shows the variation of the total phase.

Figure 4 shows the variation of the phase for several incident momenta as extracted from Arndt *et al.* [12] for various beam momenta. Also shown are values from Wallace [20] for spin-independent neutron and proton amplitudes. Wallace’s values were taken from earlier fits by Arndt’s group at lower energies. It is seen that for all cases except for the very highest beam momenta the phase increases with $q^2 = -t$ so that $a_I < 0$.

V. POTENTIAL MODELS

In this section we consider potential models for the interaction in an attempt to relate the phase to underlying physical parameters. For the Gaussian potential in the eikonal approximation we can make considerable progress analytically. We also consider the exact numerical solution for this form of potential as well as that of exponential and Woods-Saxon potential forms.

A. Gaussian potentials

In this section we assume a potential expressed as

$$V(r) = V_R e^{-r^2/r_R^2} + i V_I e^{-r^2/r_I^2}. \quad (35)$$

The integral on z in Eq. (3) can be easily done to give

$$i\chi(b) = -(\alpha e^{-b^2/r_R^2} + \beta e^{-b^2/r_I^2}), \quad (36)$$

where $\alpha = i\sqrt{\pi}r_R V_R/v = i\alpha'$ is purely imaginary and $\beta = -\sqrt{\pi}r_I V_I/v$ is real and positive (because V_I must be negative).

Now the eikonal expression is

$$\begin{aligned} f(q) &= -ik \int_0^\infty b db J_0(bq) \sum_{n=1}^\infty \frac{(-1)^n}{n!} (\alpha e^{-b^2/r_R^2} + \beta e^{-b^2/r_I^2})^n \\ &= -ik \int_0^\infty b db J_0(bq) \sum_{n=1}^\infty \frac{(-1)^n}{n!} \sum_{m=0}^n \binom{n}{m} \alpha^{n-m} \beta^m \\ &\quad \times e^{-(n-m+\eta m)b^2/r_R^2}, \end{aligned} \quad (37)$$

$$\quad (38)$$

where $\eta \equiv r_R^2/r_I^2$. Following the development in Appendix A the full expansion of the forward amplitude in powers of α is given by

$$f(0) = \frac{-ikr_I^2}{2} \left[\lambda(0, 1, \beta) + \sum_{\ell=1}^\infty \frac{(-\alpha)^\ell}{\ell!} \lambda_0 \left(\frac{\ell}{\eta}, 1, \beta \right) \right]. \quad (39)$$

We have introduced a generalization of the incomplete Gamma function with $u \geq 0$,

$$\lambda(u, k, \beta) = \sum_{n=1}^\infty \frac{(-\beta)^n}{n!(u+n)^k}. \quad (40)$$

This function can be computed from its expansion over a large part of its range. Some of its properties, including an asymptotic expansion for large final argument, are discussed in Appendix B. Another function, useful when the first argument of λ is nonzero, is

$$\lambda_0(u, k, \beta) = \sum_{n=0}^\infty \frac{(-\beta)^n}{n!(u+n)^k} = u^{-k} + \lambda(u, k, \beta). \quad (41)$$

Using Eq. (39) for $f(0)$ we can see that (to lowest order in α)

$$\rho = \alpha' \frac{\eta + \lambda(\frac{1}{\eta}, 1, \beta)}{\lambda(0, 1, \beta)}, \quad (42)$$

where $\lambda(0, 1, \beta) < 0$. The proportionality of ρ to α' shows that it is strongly influenced by the real part of the potential.

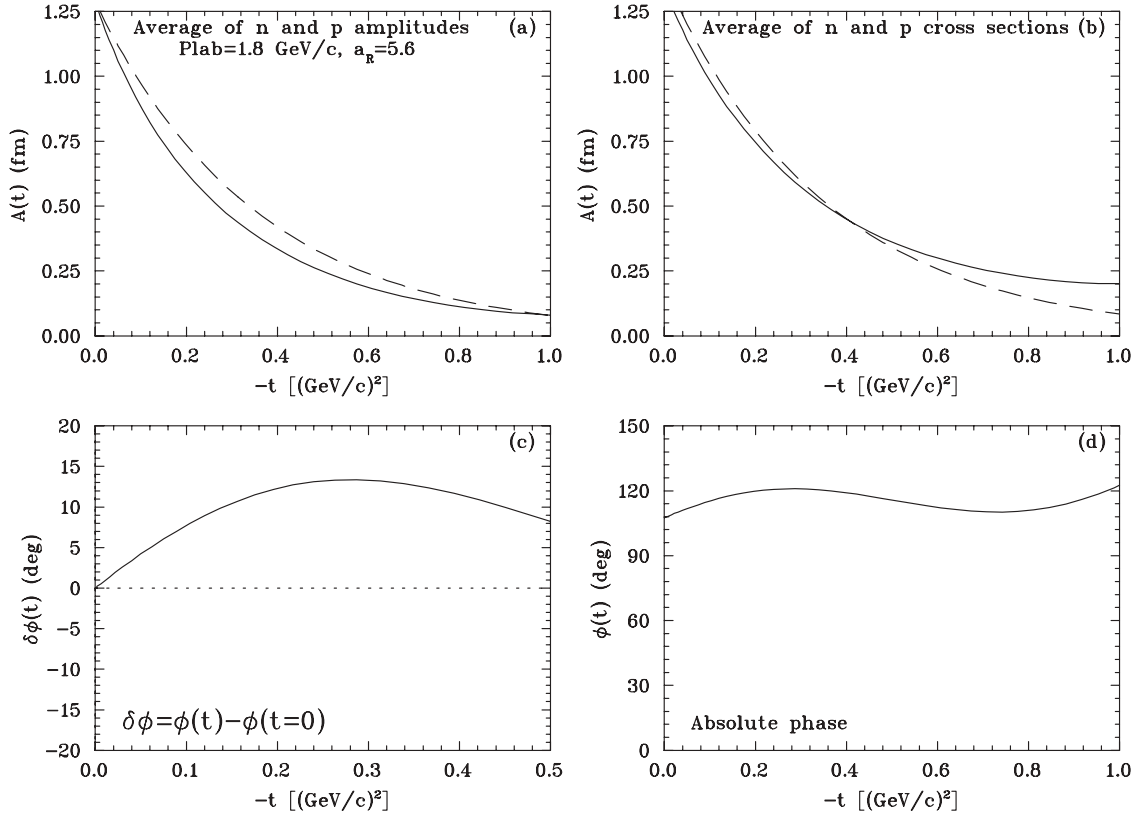


FIG. 3. Properties of the NN amplitudes at 1.8 GeV/c. Panel (a) shows the result of the absolute value of the averaged neutron and proton amplitudes. In panel (b) the solid curve shows the result of averaging the cross sections and taking the square root. In both (a) and (b) the dash curve shows a plot of the Gaussian approximation with $a_R = 5.6(\text{GeV}/c)^{-2}$. Panel (c) shows the phase relative to the phase at $t = 0$ (solid curve). Panel (d) shows the absolute phase over an extended range of t .

The total cross section, in lowest order in α , is given by

$$\sigma = 2\pi r_I^2 [g_1 + \ln(\beta) + E_1(\beta)], \quad (43)$$

where g_1 is Euler's constant. Because, for the range of values of β used here, $E_1(\beta)$ is small, the dependence of σ on β is small so that this equation provides a strong constraint on r_I . The lowest order correction in α is α^2 . This is an exact representation of the simple eikonal approximation (i.e., without corrections given by Wallace [11]) for a purely absorptive potential.

Equation (A14) can be expressed as

$$f(q) = \frac{-ikr_I^2}{2} \sum_{j=0}^{\infty} \frac{1}{j!} \left[\lambda(0, j+1, \beta) + \sum_{\ell=1}^{\infty} \frac{(-\alpha)^\ell}{\ell!} \lambda_0\left(\frac{\ell}{\eta}, j+1, \beta\right) \right] \left(\frac{-q^2 r_I^2}{4}\right)^j. \quad (44)$$

We can write the ratio to the forward amplitude [Eq. (39)] as

$$\frac{f(q)}{f(0)} = \frac{\sum_{j=0}^{\infty} \frac{1}{j!} \left[\lambda(0, j+1, \beta) + \sum_{\ell=1}^{\infty} \frac{(-\alpha)^\ell}{\ell!} \lambda_0\left(\frac{\ell}{\eta}, j+1, \beta\right) \right] \left(\frac{-q^2 r_I^2}{4}\right)^j}{\lambda(0, 1, \beta) + \sum_{\ell=1}^{\infty} \frac{(-\alpha)^\ell}{\ell!} \lambda_0\left(\frac{\ell}{\eta}, 1, \beta\right)} \quad (45)$$

so that, retaining only the first-order contribution in α' and q^2 , we have

$$\frac{f(q)}{f(0)} = 1 - \frac{r_I^2 q^2}{4} \frac{\lambda(0, 2, \beta)}{\lambda(0, 1, \beta)} \left[1 + i\alpha' \frac{\lambda_0\left(\frac{1}{\eta}, 1, \beta\right)}{\lambda(0, 1, \beta)} - i\alpha' \frac{\lambda_0\left(\frac{1}{\eta}, 2, \beta\right)}{\lambda(0, 2, \beta)} \right]. \quad (46)$$

From this expression we can identify

$$a_R + ia_I = \frac{r_I^2}{2} \frac{\lambda(0, 2, \beta)}{\lambda(0, 1, \beta)} \left\{ 1 + i\alpha' \left[\frac{\lambda_0\left(\frac{1}{\eta}, 1, \beta\right)}{\lambda(0, 1, \beta)} - \frac{\lambda_0\left(\frac{1}{\eta}, 2, \beta\right)}{\lambda(0, 2, \beta)} \right] \right\}. \quad (47)$$

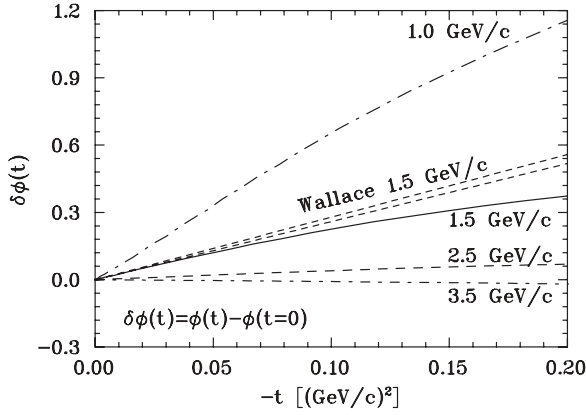


FIG. 4. Dependence of the phase on momentum transfer. The curves labeled with a momentum (P_{Lab}) are from Arndt *et al.* [12]. The two dashed curves labeled “Wallace” are the phases from neutron and proton spin-averaged amplitudes from Ref. [20].

Thus, in this linear approximation in $\alpha = i\alpha'$, we see that a_R is relatively stable under variations in the radii. However, the two ratios multiplying α' are very similar for equal radii so that a_I varies rapidly for small variations in the radii of the real and imaginary potentials.

Figure 5 shows several observables obtained from exact solutions for the Gaussian potential of as a function of the radius of the real part of the potential for $V_R = \pm 20$ MeV. The sign change of ρ and a_I with sign change of the real potential noted in the introduction in the eikonal prescription is approximately reproduced in the exact calculations.

B. Exponential potential

In this section we look at potentials of the form

$$V(r) = W_R e^{-r/c_R} + iW_I e^{-r/c_I}. \tag{48}$$

We take both W_R and W_I to be functions of the incident momentum to fit the data. We have used the phase-shift analysis of Arndt *et al.* [12] to calculate the spin-isospin average of the amplitude and used these amplitudes as a guide to fitting the potentials so we are using a spin-zero on spin-zero calculation to fit spin-averaged data. We also used the older results of Wallace [20] as well as the values of ρ from the Particle Data Group [21]. Figure 6 shows the results.

We see (solid line, direct fit) that the phase parameter a_I is negative at low incident momentum and appears to be nearing zero at higher momenta. The parameter ρ shows a similar behavior with opposite sign as expected from the simple

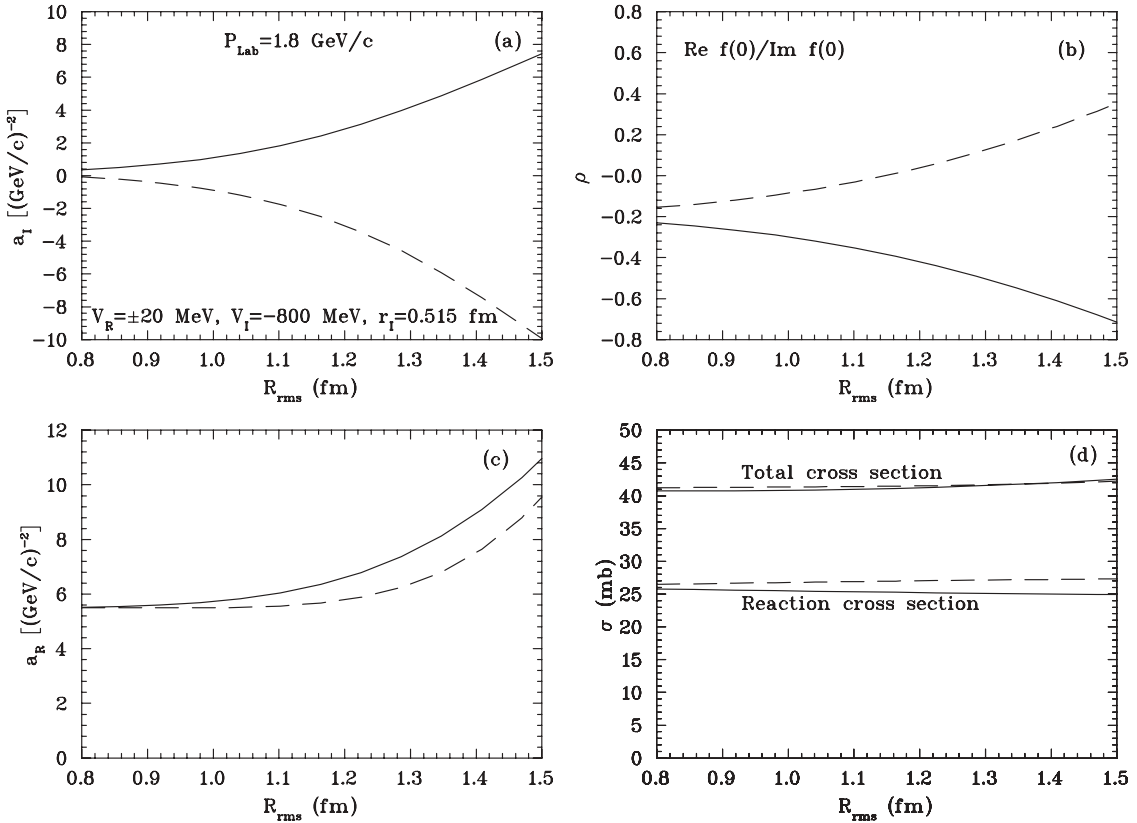


FIG. 5. Dependence of several observables on the rms radius of the real Gaussian potential well for both signs of its strength. The solid (dashed) curve shows the result for the positive (negative) potential. Panel (a) shows that the phase parameter has a very strong dependence on the radius of the real potential. In panel (b) it is seen that the ratio of real to imaginary part of the forward amplitude also has a fairly strong dependence, whereas the Gaussian parameter controlling the fall-off of the absolute value and the total and reaction cross sections have little or no dependence on this parameter.

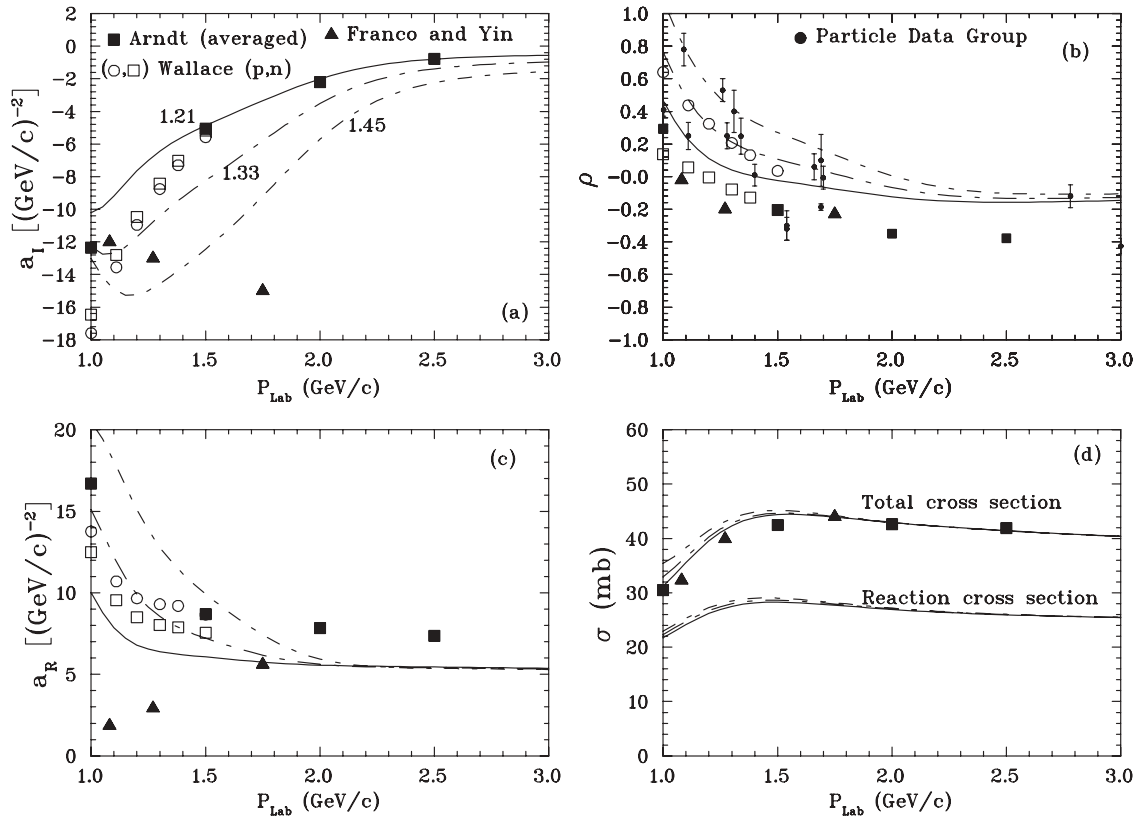


FIG. 6. Dependence of several parameters on the radius of the real potential well for the exponential potential. Panel (a) shows that the phase parameter has a very strong dependence on the radius of the real potential. The curves are labeled by the real radius (in fm). These labels identify the curves for the remaining panels as well. In panel (b) it is seen that the ratio of the real to imaginary part of the forward amplitude also has a fairly strong dependence, whereas (panels c and d) the parameter controlling the falloff of the absolute value and the total and reaction cross sections have little or no dependence on this parameter at the higher energies. The solid triangles denote the values used by Franco and Yin [3]. The open circles and squares were taken from Wallace [20]. The solid squares were extracted in the present work from the fit of Arndt *et al.* [12] and were fitted to get the solid curve. The solid dots with errors in panel (b) were taken for the Particle Data Group [21] with several points at low laboratory momentum with negative values excluded.

δ -function model of Sec. II. The parameter a_R rises slightly at low momenta and the total and reaction cross sections are relatively flat although the reaction cross section goes to zero as the momentum is reduced below 1 GeV/c.

Also shown in Fig. 6 are curves for changes from the fitted rms value for the radius of the real potential of 1.21 to 1.33 fm (dot-long dash) and 1.45 fm (dot-short dash) while holding all other parameters fixed. It is seen that there is a significant change in a_I and a corresponding change in ρ as well. There is also a more moderate (except at low momentum) change in a_R . At 2.0 GeV/c a_I goes from -2.01 to -3.52 to -5.70 $(\text{GeV}/c)^{-2}$ as the percentage change in radius goes from 0 to 10% to 20%.

C. Woods-Saxon potential

In this section we look at potentials of the form

$$V(r) = \frac{U_R}{1 + e^{(r-d_R)/p_R}} + i \frac{U_I}{1 + e^{(r-d_I)/p_I}}. \quad (49)$$

We do not believe that this form provides a realistic representation of the distribution of the strength of the interaction for the nucleon-nucleon system but we include it to show that the variation with a percentage increase in the radius of the real potential is about the same as the Gaussian or exponential potential.

Figure 7 shows results for a fit with this potential. We see that although the basic fit has a larger rms radius for the real potential than for the exponential potential, the change with percentage change in radius is qualitatively very similar. At 2.0 GeV/c a_I goes from -1.96 to -3.13 to -4.68 $(\text{GeV}/c)^{-2}$ as the percentage change in radius goes from 0 to 10% to 20%.

VI. MULTIPLE-SCATTERING RESULTS

Because multiple scattering of the projectile on a nuclear target depends on the phase of the amplitude it may be possible to measure the phase (including the phase variation) in this manner. Of course, one must be aware that what is obtained is the effective value in a nuclear medium.

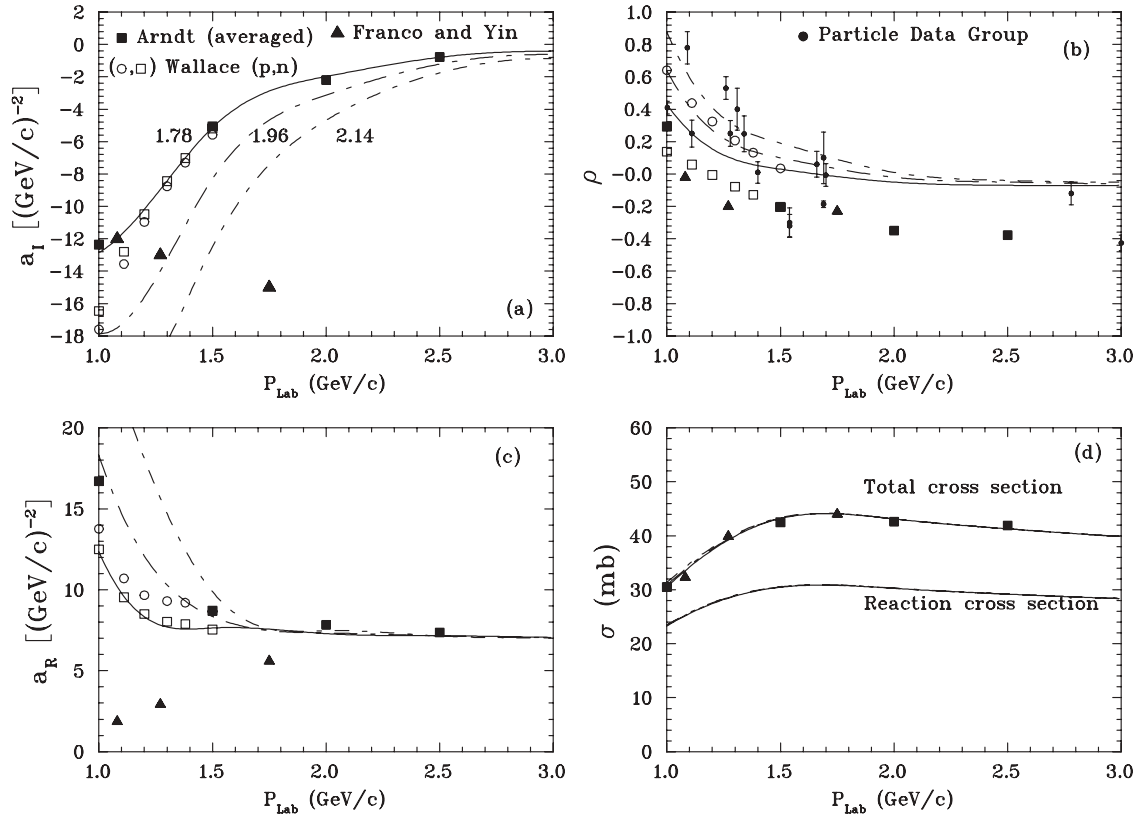


FIG. 7. Dependence of several parameters on the radius of the real potential well for the Woods-Saxon potential. Panel (a) again shows that the phase parameter has a very strong dependence on the radius of the real potential. The curves are labeled in panel (a) by the rms value of the radius of the real Woods-Saxon potential (in fm). These labels identify the curves for the remaining panels as well. The curves and symbols have the same meaning as in Fig. 6.

A. Light nuclei

Franco and Yin [3] considered the amplitude as defined in the introduction where it was assumed that only the non-spin-flip amplitude was needed for the elastic scattering on light nuclei that they considered and the variation of phase was relative to the phase at zero degrees. We follow this same definition. They pointed out that if the ratio of the real to imaginary part of the amplitude were zero, in the eikonal approximation that they used, the cross section would be independent of the sign of a_I . Because this ratio is small, but nonzero, this symmetry is only approximate and they found about the same large improvement in the agreement with data [22] for values of $+10$ and -15 $(\text{GeV}/c)^{-2}$ at 1.75 GeV/c per nucleon, $+7.5$ and -13 $(\text{GeV}/c)^{-2}$ at 1.25 GeV/c per nucleon, and $+11.5$ and -12 $(\text{GeV}/c)^{-2}$ at 1.08 GeV/c per nucleon. Clearly the values from the phase shift analyses favor the negative sign although the trend with incident momentum seems to be contrary to that seen in Ref. [3]. However, except for the 1.75 $\text{GeV}/\text{nucleon}$ case, the values of a_R are very different from those obtained from spin-averaged amplitudes (see Fig. 6 or 7). A second way to obtain the slope parameter is to fit the differential cross section with an exponential in t . In this case the spin-flip cross section is included, which leads to a more nearly isotropic cross section and hence smaller values of a_R . Thus, with this choice

some effect of the spin flip is included in the representation. The values for a_R are believed to be equivalent at about 600 MeV [23].

El-Gogary *et al.* [8] also treated α - α scattering and found (using different NN amplitude parameters) that a phase factor linear in the momentum squared of a value of $+5$ $(\text{GeV}/c)^{-2}$ greatly improved the agreement with the data at 1.75 GeV/c /nucleon.

Usmani *et al.* [7] considered the case of a modified helium wave function consisting of the sum of two Gaussian pieces. They found that for α scattering on ^4He only moderate corrections were seen. Because the data extend to a value of q^2 of 4 $(\text{GeV}/c)^2$ this may seem to be contrary to expectations. However, the $\alpha^4\text{He}$ scattering is dominated by a large number of scatterings in this momentum transfer range so that a typical value of q^2 for one of the scatterings will be reduced by a factor equal to the number of scatterings, typically between 8 and 16 . So the form factor needs to be accurate only up to a range of the order of $-t = 0.25$ – 0.5 $(\text{GeV}/c)^2$.

B. Heavier nuclei

Treating heavier nuclei, Lombard and Maillet [4] considered, in addition to the cross section, the asymmetry, A , and the spin rotation parameter, Q , so they were forced to

include the spin-dependent amplitude. Although they used for the spin-independent amplitude a basic form with no phase variation, the basic form of the spin-flip amplitude included a phase variation consistent with phase shift analyses [see their formula (2)]. The phase variation in their basic spin-flip amplitude can be represented by a coefficient of t of about $0.95 (\text{GeV}/c)^{-2}$. They then introduced a global phase variation that was applied to both amplitudes and estimated the phase parameter that would improve the agreement with the cross section and A (Q had not been measured at the time). They found that although A was not very sensitive to a variation in this phase, the quantity Q was. However, because there seems to be no reason to believe that the two amplitudes would have the same phase variation (or the difference they used), one can only conclude from their results that there is a sensitivity to the phase of the amplitudes.

Lassaut, Lombard, and Van de Wiele [5] considered an *additional* phase variation to be applied to representations of both amplitudes determined from amplitude analyses [9]. They also applied the same phase variation to both amplitudes. If one assumes that the non-spin-flip amplitude dominates the elastic cross section and adds the phase parameter they obtained [$-0.25 \text{ fm}^2 = -6.4 (\text{GeV}/c)^{-2}$] to the one present in their basic amplitudes [$-5.6 (\text{GeV}/c)^{-2}$] one arrives at a value of [$-12 (\text{GeV}/c)^{-2}$] for their incident momentum of $1.46 \text{ GeV}/c$, similar to the negative values -13 and $-15 (\text{GeV}/c)^{-2}$ obtained by Franco and Yin at nearby incident energies.

Auger and Lazard [6] considered the effect of multiplying a global phase times a parametrization of both of the nucleon amplitudes. Because they considered only asymmetry and spin rotation observables it is difficult to compare with their results. They considered phase factors with parameters close to those of Franco and Yin; however, because these must be added to the effective values already implicit in the phenomenological amplitudes they are not really comparable.

Chaumeaux *et al.* [24] also considered the addition of a phase variation in the scattering from heavier nuclei.

One expects that for all but the very lightest nuclei the sensitivity to such a phase will be small because the scattering at high energies is mainly determined by the radius and the diffuseness of the surface [25]. The influence of such a phase would mainly be contained in the region of the minima where many different multiple scattering and medium effects contribute.

C. Extracting the phase variation from multiple scattering

We have revisited the Glauber calculation of Franco and Yin [3] with a view to determine the effect of the possible nuclear modifications on the extraction of a_I from the data [22] at $1.75 \text{ GeV}/c$ /nucleon beam momentum. For helium scattering from helium it is possible to do the full multiple scattering calculation in the eikonal approximation. An additional advantage is that the basic form factor of helium has no zero in the momentum range of interest, whereas for heavier nuclei that is not true. Thus, the minima are better understood. They are not, however, simple interferences between different scattering

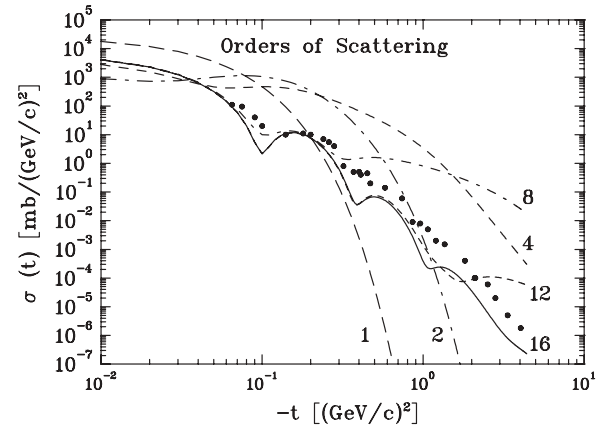


FIG. 8. Comparison of the cross section for $\alpha\alpha$ scattering calculated through various orders for $a_I = 0$ and $\rho = -0.23$. The data are from Satta *et al.* [22].

orders (as they are approximately for proton scattering on ^4He) but arise from a more complicated set of interferences. Figure 8 shows the calculation with the amplitudes obtained from the sum up to a limited number of orders for $a_I = 0$ and $\rho = -0.23$. One sees, for example, that the first minimum is well defined in position only by summing through eighth-order scattering and its depth is established by twelfth order. One also sees that the first-order scattering is negligible above about $0.6 (\text{GeV}/c)^2$. For $\rho = a_I = 0$, the individual orders of scattering are purely imaginary and alternate in sign. The effect of a finite value of ρ is to multiply the n th-order amplitude by $(1 - i\rho)^n$.

One can be concerned that the effects of ρ and a_I may be confused. The result for the full multiple scattering calculation for $\alpha\alpha$ scattering is well below the data for large q^2 , whereas in the case of the heavy nuclei, this is not in general true. There the major effect of setting a_I to a nonzero value is seen in the minima. Figure 9 shows results for variations in ρ over the uncertainty observed in the NN data. The major effect for $a_I = 0$ is to be seen only in the minima. For a finite value of a_I of $-13 (\text{GeV}/c)^{-2}$, this is not the case with the cross section away from the minima being increased as well.

In an attempt to see how well the values of a_I are determined from the α ^4He data we have calculated a χ^2 measure with regard to the data by Satta *et al.* [22]. Because no tabulated data were given we took the data from the plots including 20% errors for most points. Figure 10 shows χ^2/N for four selected values of ρ where it is seen that there are two minima. If ρ were zero, the χ^2/N curve would be symmetric. For $\rho = +0.20$ the value of about $-10 (\text{GeV}/c)^{-2}$ is favored for the negative solution.

Looking at Figs. 6 and 7 it is seen that these values of ρ and a_R might be possible by a combination of increasing the radius of the real part of the interaction and lowering the energy for the evaluation of the NN parameters although, even with these assumptions, one is at the very limit.

Before one can consider such a reconciliation of the multiple scattering and free space determinations of the phase variation there are a number of corrections that must be treated.

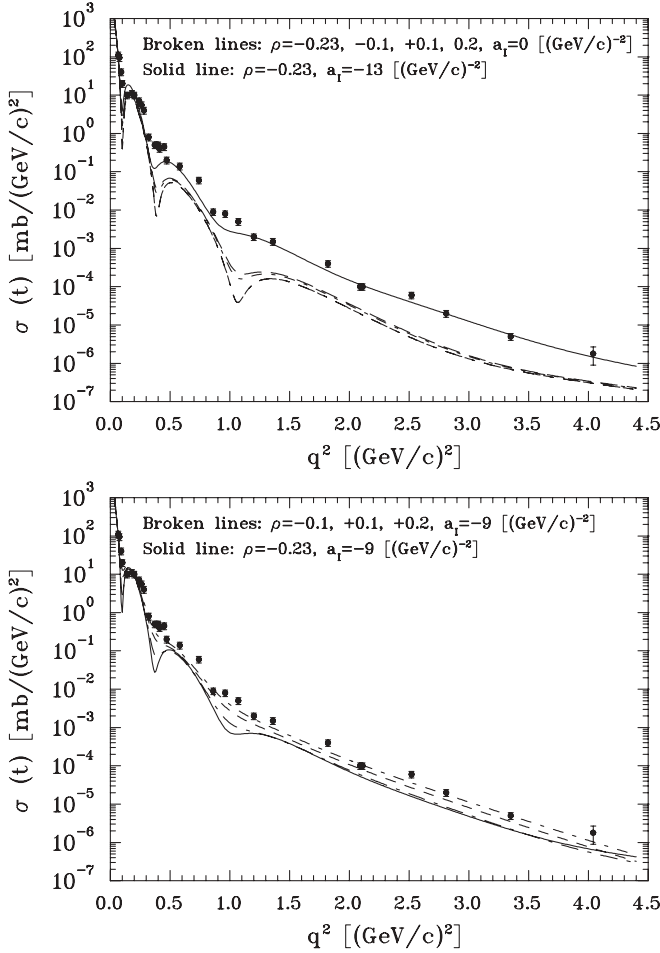


FIG. 9. Dependence of the cross section for $\alpha\alpha$ scattering on ρ and a_1 . The lower panel shows that for $\rho = 0.20$ the value of $a_1 = -9$ $(\text{GeV}/c)^{-2}$ gives an adequate fit to the data of Satta *et al.* [22].

- (i) The spin-flip may give substantial corrections through double spin flip.
- (ii) The off-shell corrections could give a contribution to the amplitude of similar nature to that of ρ and a_R .
- (iii) Short-range correlations in the ${}^4\text{He}$ wave function will modify the form factor.
- (iv) Three-body forces could affect the scattering.
- (v) Standard corrections to Glauber theory [11] still need to be considered.

This list is not meant to be exhaustive.

Of course, one is not restricted to nucleons in regard to determining the strong phase from multiple scattering. The scattering of K^+ from nuclei, as recently treated by Arellano and von Geramb [26], provides such an opportunity. They used inverse scattering theory, starting from phase shifts, to find potentials that represent the basic K^+N data. If the potentials produced represented the data but not the original phase shifts (and hence not the original phase), then ambiguities would be unearthed.

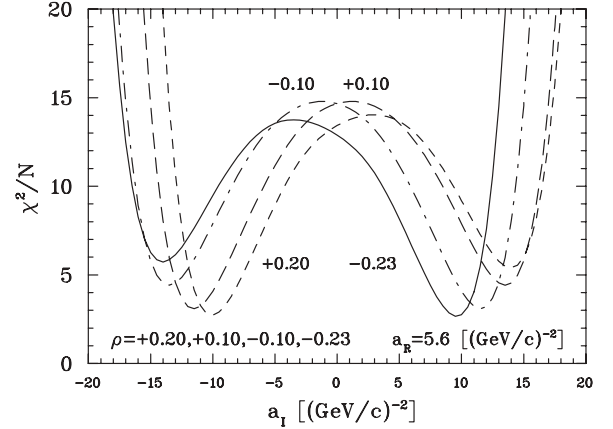


FIG. 10. Values of χ^2 from a comparison with the measured cross section for $\alpha\alpha$ scattering [22] as a function of a_1 for four different values of ρ .

VII. CONCLUSIONS

It has been shown that the phase of the strong scattering amplitude is a sensitive function of the relative size of the radii of the real and imaginary parts of a potential describing the interaction. This was done with the consideration of three models of the potential.

We have found that the phase parameter is moderately well determined for the example case of K^+p scattering from standard amplitude analyses with the controlling principle being the unitary expansion of the amplitude. It is expected that the phase in the nucleon-nucleon case would be better determined.

Because the effective amplitude in the nucleus can be taken as the free amplitude evaluated at a shifted (normally lower) energy one can perhaps understand the larger magnitude of the phase parameter than that seen in free space. Studies of this shift in the effective energy of the scattering amplitude have been made in the case of pion-nucleus scattering [27] and the predictions of such an energy shift were verified [28] experimentally. Similar corrections have been calculated in this energy range for nucleon-nucleus scattering [29].

This explanation may not be adequate to give a fit to the data so one is led to consider the possibility of a larger radius for the real part of the interaction due to a partial deconfinement in the nuclear medium. If this is true it may be a new way to study “nonclassical” modifications in the nuclear medium.

ACKNOWLEDGMENTS

This work was supported by the National Science Foundation under contract PHY-0099729.

APPENDIX A: EXPANSION OF THE NN AMPLITUDE

Starting from Eq. (38) and using

$$\int_0^\infty b db J_0(bq) e^{-d^2 b^2} = \frac{1}{2d^2} e^{-\frac{q^2}{4d^2}} \quad (\text{A1})$$

we can write

$$f(q) = -\frac{ikr_R^2}{2} \sum_{n=1}^{\infty} \frac{(-1)^n}{n!} \sum_{m=0}^n \binom{n}{m} \alpha^{n-m} \beta^m \frac{e^{-\frac{q^2 r_R^2}{4(n-m+m\eta)}}}{n-m+m\eta}. \quad (A2)$$

This equation is a generalization of Eq. 4.11 in Wallace [11] for two independent radii. In the forward direction ($q = 0$) we can write

$$f(0) = \frac{-ikr_R^2}{2} \sum_{n=1}^{\infty} \frac{(-1)^n}{n!} \sum_{m=0}^n \binom{n}{m} \alpha^{n-m} \beta^m \frac{1}{n-m+m\eta} \quad (A3)$$

or

$$\begin{aligned} f(0) &= \frac{-ikr_R^2}{2} \sum_{n=1}^{\infty} \frac{(-1)^n}{n!} \\ &\quad \times \int_0^{\infty} dt \sum_{m=0}^n \binom{n}{m} \alpha^{n-m} e^{-(n-m)t} \beta^m e^{-m\eta t} \quad (A4) \\ &= \frac{-ikr_R^2}{2} \int_0^{\infty} dt \sum_{n=1}^{\infty} \frac{(-1)^n}{n!} (\alpha e^{-t} + \beta e^{-\eta t})^n \\ &= \frac{-ikr_R^2}{2} \int_0^{\infty} dt [e^{-(\alpha e^{-t} + \beta e^{-\eta t})} - 1]. \quad (A5) \end{aligned}$$

Transforming the variable of integration from t to z with $z = e^{-\eta t}$ we have

$$f(0) = \frac{-ikr_R^2}{2\eta} \int_0^1 dz \frac{e^{-\alpha z^{\frac{1}{\eta}}} e^{-\beta z} - 1}{z}. \quad (A6)$$

Because α is thought of as smaller than β (in absolute magnitude) we expand the exponential in α to find

$$f(0) = \frac{-ikr_R^2}{2} \int_0^1 dz \frac{[(1 - \alpha z^{\frac{1}{\eta}} + \dots) e^{-\beta z} - 1]}{z} \quad (A7)$$

$$\begin{aligned} &= \frac{-ikr_R^2}{2} \left[\int_0^1 dz \frac{(e^{-\beta z} - 1)}{z} \right. \\ &\quad \left. + \sum_{\ell=1}^{\infty} \frac{(-\alpha)^{\ell}}{\ell!} \int_0^1 e^{-\beta z} z^{\frac{\ell}{\eta}-1} dz \right]. \quad (A8) \end{aligned}$$

Because

$$\int_0^1 dz \frac{(e^{-\beta z} - 1)}{z} = \sum_{n=1}^{\infty} \frac{(-\beta)^n}{n!n} = -g_1 - \ln(\beta) - E_1(\beta), \quad (A9)$$

where g_1 is Euler's constant ($= 0.57721\dots$) and $E_1(\beta)$ is the exponential integral, we have a closed form for the leading order that leads directly to Eq. (43) in the main text.

The full amplitude reads

$$\begin{aligned} f(q) &= \frac{-ikr_R^2}{2} \sum_{j=0}^{\infty} \frac{1}{(j!)^2} \left(\frac{-q^2 r_R^2}{4} \right)^j \\ &\quad \times \int_0^{\infty} t^j [e^{-(\alpha e^{-t} + \beta e^{-\eta t})} - 1] dt \quad (A10) \end{aligned}$$

and upon using the same change of variable

$$\begin{aligned} f(q) &= \frac{-ikr_I^2}{2} \sum_{j=0}^{\infty} \frac{1}{(j!)^2} \left(\frac{q^2 r_I^2}{4} \right)^j \\ &\quad \times \int_0^1 dz (\ln z)^j \frac{e^{-\beta z} e^{-\alpha z^{\frac{1}{\eta}}} - 1}{z}. \quad (A11) \end{aligned}$$

Expanding the α exponential we have

$$\begin{aligned} f(q) &= \frac{-ikr_I^2}{2} \sum_{j=0}^{\infty} \frac{1}{(j!)^2} \left(\frac{q^2 r_I^2}{4} \right)^j \int_0^1 dz (\ln z)^j \\ &\quad \times \left[\frac{e^{-\beta z} - 1}{z} + \sum_{\ell=1}^{\infty} \frac{(-\alpha)^{\ell}}{\ell!} z^{\frac{\ell}{\eta}-1} e^{-\beta z} \right] \quad (A12) \end{aligned}$$

and because

$$\int_0^1 dz (\ln z)^j z^v = \frac{(-1)^j j!}{(v+1)^{j+1}} \quad (A13)$$

we may finally write

$$\begin{aligned} f(q) &= -\frac{kr_I^2}{2} \sum_{j=0}^{\infty} \frac{1}{j!} \left[\sum_{n=1}^{\infty} \frac{(-\beta)^n}{n!n^{j+1}} + \sum_{\ell=1}^{\infty} \frac{(-\alpha)^{\ell}}{\ell!} \right. \\ &\quad \left. \times \sum_{n=0}^{\infty} \frac{(-\beta)^n}{n! \left(\frac{\ell}{\eta} + n\right)^{j+1}} \right] \left(\frac{-q^2 r_I^2}{4} \right)^j. \quad (A14) \end{aligned}$$

APPENDIX B: PROPERTIES OF THE FUNCTION λ

The power series definition of $\lambda(u, k, x)$ (40) is convergent for all values of u and x but for large values of x (greater than about 40) it is numerically difficult to calculate in that manner. We note that the relation

$$x \frac{d\lambda(0, k, x)}{dx} = \lambda(0, k-1, x) \quad (B1)$$

follows from the series definition. From this equation and from the known relation for $k=0$ and $k=1$

$$\lambda(0, 0, x) = e^{-x} - 1; \quad \lambda(0, 1, x) = -\ln(x) - g_1 - E_1(x) \quad (B2)$$

we can iterate to find the asymptotic behavior for large x .

TABLE I. Values of the coefficients g_j determined numerically (except for the first two).

0	1.000000
1	0.577215664
2	0.9890560
3	0.9074791
4	0.9817279
5	0.9819955

The asymptotic behavior of $\lambda(0, k, x)$ is given by

$$\lambda(0, k, x) \rightarrow - \sum_{i=0}^k \frac{g_{k-i} [\ln(x)]^i}{i!} \quad (\text{B3})$$

for $k \geq 0$. Note that $\lambda(0, k, x) \leq 0$ and $\lambda(0, k, x) \geq \lambda(0, k+1, x)$ for $x \geq 0$ and all $k \geq 0$.

The values of $\lambda(0, k, x)$ can be calculated to 5 significant figures with the constants given in Table I for x greater than 10

The values for x less than 40 can be easily calculated by the series.

For the variation in the first parameter, u , the relation

$$\lambda(u+1, k, x) = - \frac{d\lambda(u, k, x)}{dx} - \frac{1}{(u+1)^k} \quad (\text{B4})$$

allows the calculation the function for all values of u from those between 0 and 1. For small u we can expand the sum to get

$$\lambda(u, k, x) = \lambda(0, k, x) - ku\lambda(0, k+1, x) + \dots \quad (\text{B5})$$

-
- [1] R. H. Bassel and C. Wilkin, Phys. Rev. **174**, 1179 (1968).
 [2] J. Formanek and J. S. Trefil, Nucl. Phys. **B3**, 155 (1967).
 [3] V. Franco and Y. Yin, Phys. Rev. Lett. **55**, 1059 (1985); Phys. Rev. C **34**, 608 (1986).
 [4] R. J. Lombard and J. P. Maillet, Phys. Rev. C **41**, R1348 (1990).
 [5] M. Lassaut, R. J. Lombard, and J. Van de Wiele, J. Phys. G: Nucl. Part. Phys. **19**, 2079 (1993).
 [6] J. P. Auger and C. Lazard, J. Phys. G: Nucl. Part. Phys. **16**, 1637 (1990).
 [7] A. A. Usmani, I. Ahmad, and Q. N. Usmani, Phys. Rev. C **39**, 1182 (1989).
 [8] M. M. H. El-Gogary, A. S. Shalaby, and M. Y. M. Hassan, Phys. Rev. C **58**, 3513 (1998).
 [9] J. P. Auger, A. Tellez-Arenas, C. Lazard, and R. J. Lombard, J. Phys. G: Nucl. Part. Phys. **12**, 317 (1986).
 [10] I. Ahmad and M. A. Alvi, Phys. Rev. C **48**, 3126 (1993).
 [11] S. J. Wallace, Ann. Phys. (NY) **78**, 190 (1973).
 [12] SAID program at <http://gwdac.phys.gwu.edu>; R. A. Arndt, I. I. Strakovsky, and R. L. Workman, Phys. Rev. C **62**, 034005 (2000).
 [13] W. R. Gibbs and B. Loiseau, Phys. Rev. C **50**, 2742 (1994).
 [14] B. Loiseau, Journal de Physique, V46, Colloque 2, 339 (1985).
 [15] V. Kundrat, M. Lokajicek, and D. Krupa, Phys. Rev. D **35**, 1719 (1987).
 [16] R. B. Gerber and M. Karplus, Phys. Rev. D **1**, 998 (1979).
 [17] H. Huber, D. R. Lun, L. J. Allen, and K. Amos, Phys. Rev. A **55**, 2015 (1997).
 [18] W. R. Gibbs and R. Arceo, Phys. Rev. C **75**, 035204 (2007).
 [19] J. Bystricky, F. Lehar, and P. Winternitz, J. Phys. Lett. **40**, L117 (1979).
 [20] S. Wallace, *Advances in Nuclear Physics*, edited by J. W. Negele and E. Vogt (Plenum, New York, 1981), Vol. 12, p. 135, Tables III and IV.
 [21] W.-M. Yao *et al.*, J. Phys. G **33**, 1 (2006).
 [22] L. Satta, J. Duflo, F. Plouin, P. Picozza, L. Goldzahl, J. Banaigs, R. Frascaria, F. L. Fabbri, A. Codino, J. Berger, M. Boivin, and P. Berthet, Phys. Lett. **B139**, 263 (1984).
 [23] D. Aebischer, B. Favier, L. G. Greeniaus, R. Hess, A. Junod, C. Lechanoine, J. C. Niklès, D. Rapin, C. Richard-Serre, and D. W. Werren, Phys. Rev. D **13**, 2478 (1976).
 [24] A. Chaumeaux, V. Layly, and R. Schaeffer, Ann. Phys. (NY) **116**, 247 (1978).
 [25] R. D. Amado, J.-P. Dedonder, and F. Lenz, Phys. Rev. C **21**, 647 (1980).
 [26] H. F. Arellano and H. V. von Geramb, Phys. Rev. C **72**, 025203 (2005).
 [27] C. Schmit, Nucl. Phys. **A197**, 449 (1972); J. Revai, *ibid.* **A205**, 20 (1973); J.-P. Maillet, J.-P. Dedonder, and C. Schmit, *ibid.* **A271**, 253 (1976); **A316**, 267 (1979); M. Silver and N. Austern, Phys. Rev. C **21**, 272 (1980); H. Garcilazo and W. R. Gibbs, Nucl. Phys. **A356**, 284 (1981); J. de Kam, Phys. Rev. C **24**, 1554 (1981); W. B. Kaufmann and W. R. Gibbs, *ibid.* **28**, 1286 (1983); J.-P. Dedonder, J.-P. Maillet, and C. Schmit, Ann. Phys. (NY) **127**, 1 (1980).
 [28] W. B. Cottingham and D. B. Holtkamp, Phys. Rev. Lett. **45**, 1828 (1980).
 [29] L. Ray, Phys. Rev. C **41**, 2816 (1990).